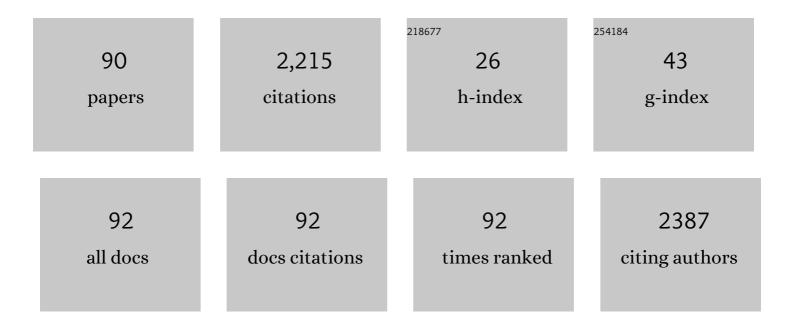
## Carolyn I Pearce

List of Publications by Year in descending order

Source: https://exaly.com/author-pdf/8664110/publications.pdf Version: 2024-02-01



#	Article	IF	CITATIONS
1	Solubility controls on plutonium and americium release in subsurface environments exposed to acidic processing wastes. Applied Geochemistry, 2023, 153, 105241.	3.0	0
2	<sup>27</sup> Al NMR diffusometry of Al <sub>13</sub> Keggin nanoclusters. Magnetic Resonance in Chemistry, 2022, 60, 226-238.	1.9	3
3	Extending Zavitsas' hydration model to the thermodynamics of solute mixtures in water. Journal of Molecular Liquids, 2022, 347, 118309.	4.9	6
4	Sorption of Strontium to Uraninite and Uranium(IV)–Silicate Nanoparticles. Langmuir, 2022, 38, 3090-3097.	3.5	3
5	A Review of Bismuth(III)-Based Materials for Remediation of Contaminated Sites. ACS Earth and Space Chemistry, 2022, 6, 883-908.	2.7	6
6	Radiolysis and Radiation-Driven Dynamics of Boehmite Dissolution Observed by In Situ Liquid-Phase TEM. Environmental Science & Technology, 2022, 56, 5029-5036.	10.0	8
7	Pu distribution among mixed waste components at the Hanford legacy site, USA and implications to long-term migration. Applied Geochemistry, 2022, , 105304.	3.0	4
8	Assessment of the reason for the vitrification of a wall at a hillfort. The example of Broborg in Sweden. Journal of Archaeological Science: Reports, 2022, 43, 103459.	0.5	1
9	Ion hydration controls self-diffusion in multicomponent aqueous electrolyte solutions of NaNO2-NaOH-H2O. Journal of Molecular Liquids, 2022, 360, 119441.	4.9	3
10	Hydroxide promotes ion pairing in the NaNO <sub>2</sub> –NaOH–H <sub>2</sub> O system. Physical Chemistry Chemical Physics, 2021, 23, 112-122.	2.8	8
11	Niche Partitioning of Microbial Communities at an Ancient Vitrified Hillfort: Implications for Vitrified Radioactive Waste Disposal. Geomicrobiology Journal, 2021, 38, 36-56.	2.0	5
12	Reproduction of melting behavior for vitrified hillforts based on amphibolite, granite, and basalt lithologies. Scientific Reports, 2021, 11, 1272.	3.3	9
13	Photon-In/Photon-Out X-ray Free-Electron Laser Studies of Radiolysis. Applied Sciences (Switzerland), 2021, 11, 701.	2.5	1
14	Influences on Subsurface Plutonium and Americium Migration. ACS Earth and Space Chemistry, 2021, 5, 279-294.	2.7	4
15	Nitrate and nitrite incompatibility with hydroxide ions in concentrated NaOH solutions: Implications for hydroxide and gibbsite reactivity in alkaline nuclear waste. Fluid Phase Equilibria, 2021, 532, 112922.	2.5	5
16	Crystallization and Phase Transformations of Aluminum (Oxy)hydroxide Polymorphs in Caustic Aqueous Solution. Inorganic Chemistry, 2021, 60, 9820-9832.	4.0	15
17	Cluster defects in gibbsite nanoplates grown at acidic to neutral pH. Nanoscale, 2021, 13, 17373-17385.	5.6	5
18	The controlling role of atmosphere in dawsonite <i>versus</i> gibbsite precipitation from tetrahedral aluminate species. Dalton Transactions, 2021, 50, 13438-13446.	3.3	1

#	Article	IF	CITATIONS
19	Molecular Examination of Ion-Pair Competition in Alkaline Aluminate Solutions Using In Situ Liquid SIMS. Analytical Chemistry, 2021, 93, 1068-1075.	6.5	6
20	Theory-Guided Inelastic Neutron Scattering of Crystalline Alkaline Aluminate Salts Bearing Principal Motifs of Solution-State Species. Inorganic Chemistry, 2021, 60, 16223-16232.	4.0	4
21	Applying laboratory methods for durability assessment of vitrified material to archaeological samples. Npj Materials Degradation, 2021, 5, .	5.8	5
22	Forty years of durability assessment of nuclear waste glass by standard methods. Npj Materials Degradation, 2021, 5, .	5.8	35
23	Iodine immobilization by materials through sorption and redox-driven processes: A literature review. Science of the Total Environment, 2020, 716, 132820.	8.0	59
24	Technetium immobilization by materials through sorption and redox-driven processes: A literature review. Science of the Total Environment, 2020, 716, 132849.	8.0	19
25	Ion–ion interactions enhance aluminum solubility in alkaline suspensions of nano-gibbsite (α-Al(OH) <sub>3</sub> ) with sodium nitrite/nitrate. Physical Chemistry Chemical Physics, 2020, 22, 4368-4378.	2.8	19
26	Evaluation of materials for iodine and technetium immobilization through sorption and redox-driven processes. Science of the Total Environment, 2020, 716, 136167.	8.0	16
27	Labile Fe(III) from sorbed Fe(II) oxidation is the key intermediate in Fe(II)-catalyzed ferrihydrite transformation. Geochimica Et Cosmochimica Acta, 2020, 272, 105-120.	3.9	72
28	Mechanisms of Al <sup>3+</sup> Dimerization in Alkaline Solutions. Inorganic Chemistry, 2020, 59, 18181-18189.	4.0	8
29	Influence of soluble oligomeric aluminum on precipitation in the Al–KOH–H2O system. Physical Chemistry Chemical Physics, 2020, 22, 24677-24685.	2.8	7
30	Characterization of Glass Alterations in Ancient Glass from Various Environments from Broborg, a Vitrified Swedish Hillfort. Microscopy and Microanalysis, 2020, 26, 2592-2593.	0.4	2
31	Nanoscale observations of Fe( <scp>ii</scp> )-induced ferrihydrite transformation. Environmental Science: Nano, 2020, 7, 2953-2967.	4.3	21
32	Longâ€ŧerm accumulation, depth distribution, and speciation of silver nanoparticles in biosolidsâ€amended soils. Journal of Environmental Quality, 2020, 49, 1679-1689.	2.0	6
33	Solid-State Recrystallization Pathways of Sodium Aluminate Hydroxy Hydrates. Inorganic Chemistry, 2020, 59, 6857-6865.	4.0	11
34	Hybrid Sorbents for <sup>129</sup> I Capture from Contaminated Groundwater. ACS Applied Materials & Interfaces, 2020, 12, 26113-26126.	8.0	19
35	Al27 NMR chemical shift of Al(OH)4â^' calculated from first principles: Assessment of error cancellation in chemically distinct reference and target systems. Journal of Chemical Physics, 2020, 152, 134303.	3.0	3
36	Polystyrene nano- and microplastic accumulation at Arabidopsis and wheat root cap cells, but no evidence for uptake into roots. Environmental Science: Nano, 2020, 7, 1942-1953.	4.3	102

#	Article	IF	CITATIONS
37	Two-step route to size and shape controlled gibbsite nanoplates and the crystal growth mechanism. CrystEngComm, 2020, 22, 2555-2565.	2.6	10
38	Kinetics of Co-Mingled <sup>99</sup> Tc and Cr Removal during Mineral Transformation of Ferrous Hydroxide. ACS Earth and Space Chemistry, 2020, 4, 218-228.	2.7	5
39	Effect of Cr(III) Adsorption on the Dissolution of Boehmite Nanoparticles in Caustic Solution. Environmental Science & Technology, 2020, 54, 6375-6384.	10.0	8
40	Intermediate Species in the Crystallization of Sodium Aluminate Hydroxy Hydrates. Journal of Physical Chemistry C, 2020, 124, 12337-12345.	3.1	10
41	Inference of principal species in caustic aluminate solutions through solid-state spectroscopic characterization. Dalton Transactions, 2020, 49, 5869-5880.	3.3	10
42	The role of surface hydroxyls on the radiolysis of gibbsite and boehmite nanoplatelets. Journal of Hazardous Materials, 2020, 398, 122853.	12.4	18
43	Silicate stabilisation of colloidal UO2 produced by uranium metal corrosion. Journal of Nuclear Materials, 2019, 526, 151751.	2.7	10
44	Structure, Magnetism, and the Interaction of Water with Ti-Doped Fe3O4 Surfaces. Langmuir, 2019, 35, 13872-13879.	3.5	6
45	A Closer Look at Fe(II) Passivation of Goethite. ACS Earth and Space Chemistry, 2019, 3, 2717-2725.	2.7	22
46	Transformation of Gibbsite to Boehmite in Caustic Aqueous Solution at Hydrothermal Conditions. Crystal Growth and Design, 2019, 19, 5557-5567.	3.0	19
47	Cr(III) Adsorption by Cluster Formation on Boehmite Nanoplates in Highly Alkaline Solution. Environmental Science & Technology, 2019, 53, 11043-11055.	10.0	42
48	Unraveling Gibbsite Transformation Pathways into LiAl-LDH in Concentrated Lithium Hydroxide. Inorganic Chemistry, 2019, 58, 12385-12394.	4.0	29
49	Redistribution of Electron Equivalents between Magnetite and Aqueous Fe2+ Induced by a Model Quinone Compound AQDS. Environmental Science & Technology, 2019, 53, 1863-1873.	10.0	18
50	Resolving local configurational contributions to X-ray and neutron radial distribution functions within solutions of concentrated electrolytes – a case study of concentrated NaOH. Physical Chemistry Chemical Physics, 2019, 21, 6828-6838.	2.8	14
51	Countercations Control Local Specific Bonding Interactions and Nucleation Mechanisms in Concentrated Water-in-Salt Solutions. Journal of Physical Chemistry Letters, 2019, 10, 3318-3325.	4.6	19
52	Radiation Damage Effects in Chlorite Investigated Using Microfocus Synchrotron Techniques. ACS Earth and Space Chemistry, 2019, 3, 652-662.	2.7	0
53	Interactions of HCl and H2O with the surface of PuO2. Journal of Nuclear Materials, 2019, 518, 256-264.	2.7	8
54	Successful Decontamination of <sup>99</sup> TcO <sub>4</sub> <sup>â^'</sup> in Groundwater at Legacy Nuclear Sites by a Cationic Metalâ€Organic Framework with Hydrophobic Pockets. Angewandte Chemie - International Edition, 2019, 58, 4968-4972.	13.8	177

#	Article	IF	CITATIONS
55	Successful Decontamination of <sup>99</sup> TcO <sub>4</sub> <sup>â^`</sup> in Groundwater at Legacy Nuclear Sites by a Cationic Metalâ€Organic Framework with Hydrophobic Pockets. Angewandte Chemie, 2019, 131, 5022-5026.	2.0	37
56	Surface speciation and interactions between adsorbed chloride and water on cerium dioxide. Journal of Solid State Chemistry, 2018, 262, 16-25.	2.9	5
57	Anticorrelated Contributions to Pre-edge Features of Aluminate Near-Edge X-ray Absorption Spectroscopy in Concentrated Electrolytes. Journal of Physical Chemistry Letters, 2018, 9, 2444-2449.	4.6	9
58	Radiolytic stability of gibbsite and boehmite with adsorbed water. Journal of Nuclear Materials, 2018, 501, 224-233.	2.7	30
59	The Role of Defects in Fe(II)–Goethite Electron Transfer. Environmental Science & Technology, 2018, 52, 2751-2759.	10.0	76
60	Size and Morphology Controlled Synthesis of Boehmite Nanoplates and Crystal Growth Mechanisms. Crystal Growth and Design, 2018, 18, 3596-3606.	3.0	82
61	Preâ€Viking Swedish hillfort glass: A prospective longâ€term alteration analogue for vitrified nuclear waste. International Journal of Applied Glass Science, 2018, 9, 540-554.	2.0	13
62	Getters for improved technetium containment in cementitious waste forms. Journal of Hazardous Materials, 2018, 341, 238-247.	12.4	25
63	<sup>27</sup> Al Pulsed Field Gradient, Diffusion–NMR Spectroscopy of Solvation Dynamics and Ion Pairing in Alkaline Aluminate Solutions. Journal of Physical Chemistry B, 2018, 122, 10907-10912.	2.6	15
64	Coupled Multimodal Dynamics of Hydrogen-Containing Ion Networks in Water-Deficient, Sodium Hydroxide-Aluminate Solutions. Journal of Physical Chemistry B, 2018, 122, 12097-12106.	2.6	12
65	Boehmite and Cibbsite Nanoplates for the Synthesis of Advanced Alumina Products. ACS Applied Nano Materials, 2018, 1, 7115-7128.	5.0	79
66	Cr(VI) Effect on Tc-99 Removal from Hanford Low-Activity Waste Simulant by Ferrous Hydroxide. Environmental Science & Technology, 2018, 52, 11752-11759.	10.0	11
67	Characterizing Technetium in Subsurface Sediments for Contaminant Remediation. ACS Earth and Space Chemistry, 2018, 2, 1145-1160.	2.7	8
68	Ab Initio Molecular Dynamics Reveal Spectroscopic Siblings and Ion Pairing as New Challenges for Elucidating Prenucleation Aluminum Speciation. Journal of Physical Chemistry B, 2018, 122, 7394-7402.	2.6	34
69	In Situ <sup>27</sup> Al NMR Spectroscopy of Aluminate in Sodium Hydroxide Solutions above and below Saturation with Respect to Gibbsite. Inorganic Chemistry, 2018, 57, 11864-11873.	4.0	33
70	Stability, Composition, and Core–Shell Particle Structure of Uranium(IV)-Silicate Colloids. Environmental Science & Technology, 2018, 52, 9118-9127.	10.0	21
71	Technetium Stabilization in Low-Solubility Sulfide Phases: A Review. ACS Earth and Space Chemistry, 2018, 2, 532-547.	2.7	36
72	Characterisation and heat treatment of chloride-contaminated and humidified PuO2 samples. Journal of Nuclear Materials, 2018, 509, 654-666.	2.7	10

#	Article	IF	CITATIONS
73	Spectroscopic Characterization of Aqua [ <i>fac</i> -Tc(CO) <sub>3</sub> ] <sup>+</sup> Complexes at High Ionic Strength. Inorganic Chemistry, 2018, 57, 6903-6912.	4.0	10
74	Reversible Fe( <scp>ii</scp> ) uptake/release by magnetite nanoparticles. Environmental Science: Nano, 2018, 5, 1545-1555.	4.3	20
75	Impact of Ti Incorporation on Hydroxylation and Wetting of Fe <sub>3</sub> O <sub>4</sub> . Journal of Physical Chemistry C, 2017, 121, 19288-19295.	3.1	10
76	First-Principles Fe L <sub>2,3</sub> -Edge and O K-Edge XANES and XMCD Spectra for Iron Oxides. Journal of Physical Chemistry A, 2017, 121, 7613-7618.	2.5	30
77	Transitions in Al Coordination during Gibbsite Crystallization Using High-Field <sup>27</sup> Al and <sup>23</sup> Na MAS NMR Spectroscopy. Journal of Physical Chemistry C, 2017, 121, 27555-27562.	3.1	41
78	Fast Synthesis of Gibbsite Nanoplates and Process Optimization using Box-Behnken Experimental Design. Crystal Growth and Design, 2017, 17, 6801-6808.	3.0	47
79	Reduction and Simultaneous Removal of <sup>99</sup> Tc and Cr by Fe(OH) <sub>2</sub> (s) Mineral Transformation. Environmental Science & Technology, 2017, 51, 8635-8642.	10.0	68
80	Tc(VII) and Cr(VI) Interaction with Naturally Reduced Ferruginous Smectite from a Redox Transition Zone. Environmental Science & Technology, 2017, 51, 9042-9052.	10.0	38
81	Radiation damage in biotite mica by accelerated α-particles: A synchrotron microfocus X-ray diffraction and X-ray absorption spectroscopy studyk. American Mineralogist, 2016, 101, 928-942.	1.9	7
82	Incorporation of Technetium into Spinel Ferrites. Environmental Science & Technology, 2016, 50, 13160-13168.	10.0	32
83	Redox cycling of Fe(II) and Fe(III) in magnetite by Fe-metabolizing bacteria. Science, 2015, 347, 1473-1476.	12.6	239
84	Magnetization Measurements and XMCD Studies on Ion Irradiated Iron Oxide and Core-Shell Iron/Iron-Oxide Nanomaterials. IEEE Transactions on Magnetics, 2014, 50, 1-5.	2.1	9
85	Fe <sub>3–<i>x</i></sub> Ti <sub><i>x</i></sub> O <sub>4</sub> Nanoparticles as Tunable Probes of Microbial Metal Oxidation. Journal of the American Chemical Society, 2013, 135, 8896-8907.	13.7	43
86	Reaction of U <sup>VI</sup> with Titanium-Substituted Magnetite: Influence of Ti on U <sup>IV</sup> Speciation. Environmental Science & Technology, 2013, 47, 4121-4130.	10.0	30
87	Thermodynamics of the magnetite-ulvospinel (Fe3O4-Fe2TiO4) solid solution. American Mineralogist, 2012, 97, 1330-1338.	1.9	45
88	Fe site occupancy in magnetite-ulvospinel solid solutions: A new approach using X-ray magnetic circular dichroism. American Mineralogist, 2010, 95, 425-439.	1.9	75
89	Isotopic Substitution Reveals the Importance of Aluminate Diffusion Dynamics in Gibbsite (Al(OH) <sub>3</sub> ) Crystallization from Alkaline Aqueous Solution. ACS Earth and Space Chemistry, 0, , .	2.7	1
90	Sodium site occupancy and phosphate speciation in natrophosphate are invariant to changes in NaF and Na <sub>3</sub> PO <sub>4</sub> concentration. Inorganic Chemistry Frontiers, 0, , .	6.0	1